

Age-Dependent Loss of Sperm Production in Mice via Impaired Lysophosphatidic Acid Signaling¹

Xiaoqin Ye,^{3,4} Michael K. Skinner,⁵ Grace Kennedy,⁴ and Jerold Chun^{2,4}

Department of Molecular Biology,⁴ The Helen L. Dorris Child and Adolescent Neuropsychiatric Disorder Institute, The Scripps Research Institute, La Jolla, California 92037
Center for Reproductive Biology,⁵ School of Molecular Bioscience, Washington State University, Pullman, Washington 99164-4231

ABSTRACT

Approximately half of all infertility cases can be attributed to male reproductive dysfunction for which low sperm count is a major contributing factor. The current study identified receptor-mediated lysophosphatidic acid (LPA) signaling as a new molecular component influencing male fertility. LPA is a small signaling phospholipid, the effects of which are mediated through at least five G protein-coupled receptors, named LPA 1–5. LPA1/2/3, but not LPA4/5, show high expression in mouse testis. Mice deficient in LPA1/2/3 showed a testosterone-independent reduction of mating activity and sperm production, with an increased prevalence of azoospermia in aging animals. A significant increase of germ cell apoptosis also was observed in testes. Germ cell apoptosis led to a reduction in germ cell proliferation. These data demonstrate a novel *in vivo* function for LPA signaling as a germ cell survival factor during spermatogenesis.

germ cell apoptosis and proliferation, LPA and S1P, sperm count, spermatogenesis, testis

INTRODUCTION

The small lipid signaling molecule lysophosphatidic acid (LPA; 1-acyl-2-*sn*-glycerol-3-phosphate) can be found at micromolar concentrations in serum and can be produced by many cell types, such as activated platelets, erythrocytes, leukocytes, postmitotic neurons, adipocytes, and ovarian cancer cells [1–7]. LPA is produced by the enzymes ectonucleotide lysophosphatase/phosphodiesterase 2 (ENPP2; lysophospholipase D, autotaxin/lysoPLD) and/or phospholipases A1 and A2 (PLA1 and PLA2, respectively) [6, 8]. Extracellular signaling by LPA is mediated predominantly by at least five cognate G protein-coupled receptors, known as LPA 1–5 (LPA1/EDG2/*vz*g-1, LPA2/EDG4, LPA3/EDG7, LPA4/GPR23, and LPA5/GPR92) [1, 9, 10], to produce a range of cellular effects, such as proliferation, survival, differentiation, and morphological changes.

¹Supported by National Institutes of Health grant R01 HD050685 to J.C.

²Correspondence: Jerold Chun, Department of Molecular Biology, ICND 118, The Scripps Research Institute, 10550 North Torrey Pines Road, La Jolla, CA 92037. FAX: 858 784 7084; e-mail: jchun@scripps.edu

³Current address: Department of Physiology and Pharmacology, College of Veterinary Medicine, and Interdisciplinary Toxicology Program, University of Georgia, Athens, GA 30602.

Received: 29 February 2008.

First decision: 24 March 2008.

Accepted: 8 April 2008.

© 2008 by the Society for the Study of Reproduction, Inc.

ISSN: 0006-3363. <http://www.biolreprod.org>

Signaling by LPA has important roles in many organ systems, including the female reproductive system [1, 8, 11–16], which uses LPA3 signaling [17]. Previous studies have reported LPA biosynthetic enzymes, including PLA1, PLA2, and ENPP2 [6, 18–22], as well as LPA receptor gene expression in the testis [23]. Single receptor-null mutants for *Lpar1*, *Lpar2*, or *Lpar3* have not shown obvious male reproductive defects [17, 24, 25]. On closer inspection, however, small reductions in sperm production have been documented, suggesting that deletion of multiple LPA receptors might unmask compensatory mechanisms. To address this possibility, we generated a mouse mutant deficient for three LPA receptors, LPA1/2/3.

MATERIALS AND METHODS

Generation of Mutant Mice

Lpar1^(-/-) (*Lpar1*^{tm1Jch}), *Lpar2* (*Lpar2*^{tm1Jch(-/-)}), *Lpar1*^(-/-)*Lpar2*^(-/-) (*Lpar1*^{tm1Jch}*Lpar2*^{tm1Jch}), and *Lpar3*^(-/-) (*Lpar3*^{tm1Jch}) knockout mice were generated as described previously [17, 24, 25]. *Lpar1*^(-/-)*Lpar3*^(-/-) (*Lpar1*^{tm1Jch}*Lpar3*^{tm1Jch}), *Lpar2*^(-/-)*Lpar3*^(-/-) (*Lpar2*^{tm1Jch}*Lpar3*^{tm1Jch}), and *Lpar1/2/3* (*Lpar1*^{tm1Jch}*Lpar2*^{tm1Jch}*Lpar3*^{tm1Jch}) triple-knockout (TKO) mice were generated by crossing single- and/or double-knockout mice. Each knockout mouse was subjected to genotyping for *Lpar1*, *Lpar2*, and *Lpar3* alleles as described previously [17, 24, 25]. All analyses reported here regarding knockout and wild-type (WT) mice were from animals with a mixed 129/SvJ and C57BL/6 background unless otherwise specified. All the animals were generated and maintained in the laboratory of one of the authors (J.C.) at the University of California, San Diego, and later at The Scripps Research Institute. All animal research conducted for the present study was approved by the Animal Subjects Committee of The Scripps Research Institute and conformed to National Institutes of Health guidelines and public law.

Real-Time RT-PCR

Three WT males (age, 4 wk; C57BL/6) were anesthetized by isoflurane inhalation. Testes were immediately removed and snap-frozen in liquid nitrogen. Total RNA was isolated using Trizol (Gibco BRL) following the manufacturer's instructions except that each sample was extracted twice with chloroform. The RNA samples were analyzed by gel electrophoresis to confirm their integrity and the absence of chromosomal DNA contamination. Complementary DNA was transcribed from 1 µg of total RNA using Superscript II reverse transcriptase (Invitrogen) with random primers. Real-time PCR reactions were performed using SYBR Green intercalating dye (Sigma) on a Rotor-Gene 3000 (Corbett Research). The relative transcript number of each gene was quantified and normalized to actin, beta, cytoplasmic (*Actb*). Each primer pair crosses intron(s) in genomic DNA. The following primer pairs, with the expected product size indicated, were used for each gene: LPA1e3F1, 5'-TCT TCT GGG CCA TTT TCA AC-3', and LPA1e4R1, 5'-TGC CTG AAG GTG GCG CTC AT-3' (*Lpar1*, 350 bp); LPA2e2F1, 5'-ACC ACA CTC AGC CTA GTC AAG AC-3', and LPA2e3R1, 5'-CTG AGT AAC GGG CAG ACT TG-3' (*Lpar2*, 277 bp); LPA3e2F2, 5'-ACA CCA GTG GCT CCA TCA G-3', and LPA3e3R2, 5'-GTT CAT GAC GGA GTT GAG CAG-3' (*Lpar3*, 201 bp); LPA4e1F1, 5'-AGG CAT GAG CAC ATT CTC TC-3', and LPA4e2R1, 5'-CAA CCT GGG TCT GAG ACT TG-3' (*Lpar4*, 292 bp); LPA5e1F1, 5'-AGG AAG AGC AAC CGA TCA TCA CAG-3', and

LPA5e2R1, 5'-ACC ACC ATA TGC AAA CGA TGT G-3' (*Lpar5*, 335 bp); Actbe5F1, 5'-TGG AAT CCT GTG GCA TCC ATG AAA C-3', and Actbe6R1, 5'-TAA AAC GCA GCT CAG TAA CAG TCC G-3' (actin, beta, cytoplasmic, 349 bp).

In Situ Hybridization

Testes were removed from anesthetized WT males at the ages of 15 days, 4 wk, and 4 mo and immediately frozen in Tissue-Tek optimal cutting temperature (OCT) compound with dry ice (Miles, Elkhart, IN). The frozen testes were kept at -80°C . Cross-sections (thickness, 20 μm) were cut and processed as described previously [26, 27]. The sections were hybridized with digoxigenin-labeled sense or antisense riboprobes, which were transcribed from linearized plasmids containing coding regions of mouse *Lpar1/2/3* using T3 or T7 RNA polymerases. The hybridization was visualized by an alkaline phosphatase-conjugated anti-digoxigenin antibody (Roche).

Histology

Mice at 0, 15, and 28 days as well as 6 mo of age were anesthetized by isoflurane inhalation. Testes were immediately removed and fixed in Bouin solution (Sigma) overnight. Each testis was cut perpendicular to the long axis of the seminiferous tubules. Paraffin sections (thickness, 5 μm) were cut, processed, and stained with hematoxylin and eosin.

Mating Study

Wild-type or *Lpar1/2/3* TKO males (age, 10–12 wk) and C57BL/6 virgin females (age, 8 wk) were used in the natural mating study. Three females were placed with each male and were checked for vaginal plugs every morning. Once a vaginal plug was found, the female was removed and placed in a separate cage. All nonplugged females were separated from males after 1 mo of cohabitation and were observed for at least 3 wk. In addition, *Lpar1/2/3* TKO females (age, 2–6 mo) were mated with WT males (age, 2–4 mo) to determine litter sizes. Litter size was calculated as the total number of pups found at Postnatal Day 0.

Sperm Count

Males were housed alone for 1 wk before they were killed. Both cauda epididymes were removed, weighed, and finely diced in 1 ml of 37°C Ringer buffer with 0.05% BSA in a 1.5-ml microcentrifuge tube, then shaken at 37°C for 30 min. Each sample was counted three times using a hemocytometer and quantified. No difference in the weight of cauda epididymes was observed between WT and *Lpar1/2/3* TKO mice.

Serum Testosterone Measurement

Serum testosterone levels were measured by standard radioimmunoassay according to the manufacturer's instructions (Diagnostic Systems Laboratory, Inc.).

MAPK3/1 Kinase Assay

Testes from 2-mo-old males ($n = 3\text{--}4$ mice/group) were removed and placed in a Petri dish containing serum-free Dulbecco Modified Eagle Medium (DMEM)/F12 medium (Gibco). The tunica albuginea was quickly removed, and the seminiferous tubules were immediately transferred to a 1.5-ml centrifuge tube in which they were minced. The cell suspension was filtered through nylon mesh (pore size, 100 μm ; Beckman) into a 50-ml Falcon tube and centrifuged ($900 \times g$, 5 min, room temperature). The cells were washed again with serum-free DMEM/F12 medium and cultured under serum-free conditions overnight at 32°C. The medium was then replaced with fresh medium containing variable concentrations of LPA (Avanti Polar Lipids) or sphingosine 1-phosphate (Avanti Polar Lipids) dissolved in 0.1% fatty acid-free BSA. Cells were incubated at 32°C for 10–60 min before they were harvested for protein extraction. Protein preparations and kinase assays were done as described previously [25, 28]. Primary antibodies to MAPK3/1 (extracellular regulated kinases 2/1, also known as ERK2/1) and phospho-MAPK3/1 (1:1,000; Cell Signal) were used in the present study.

5-Bromo-3-Deoxyuridine Labeling and In Situ End-Labeling Plus Detection

Wild-type, *Lpar3*^(+/-) (as a control), and *Lpar1/2/3* TKO mice at 15 days, 3 mo, and 8 mo of age were injected intraperitoneally with 5-bromo-3-

deoxyuridine (BrdU; 20 $\mu\text{l/g}$ body weight, 10 mM in 1 \times PBS) 2 h before death. Testes were immediately removed and freshly frozen in M-1 embedding compound (Thermo Shandon). Cross-sections (thickness, 20 μm) were processed for BrdU immunolabeling and in situ end-labeling plus (ISEL⁺), performed as described previously [29–31], using a Cy5-conjugated anti-BrdU (red) primary antibody. Semiquantification of germ cell proliferation was performed in seminiferous tubules arbitrarily divided into the following five groups based on the percentage of BrdU-labeled germ cells: 0%, no labeling; less than 5%, sparsely labeled; 5–30%, low level of labeling; 30–70%, medium level of labeling; and greater than 70%, high level of labeling. All the tubules in the whole-testis section were given a score and tallied.

Data Representation

Data are expressed as the mean \pm SD or SEM as indicated. Statistical analyses were done using the Student *t*-test, two-sample rank testing, or chi-square test. The significance level was set at $P < 0.05$.

RESULTS

Expression of LPA Receptors in Mouse Testis

It has been demonstrated previously by Northern blot analysis that the transcripts of *Lpar1*, *Lpar2*, and *Lpar3*, but not those of *Lpar4* and *Lpar5*, are highly detectable in the testis [9, 23, 32]. We quantified mRNA expression levels of the five LPA receptors at 4 wk of age, which demonstrated *Lpar1*, *Lpar2*, and *Lpar3* levels of 3,200- to more than 10,000-fold higher than those of *Lpar4* or *Lpar5* in the testis (Fig. 1a); therefore, we focused our analyses on LPA1, LPA2, and LPA3. In situ hybridization studies (Fig. 1b) revealed gene expression of these three receptors in seminiferous tubules at all ages examined. At 15 days of age, *Lpar1* mRNA was detected in the periphery of all seminiferous tubules, overlapping with a similar pattern for *Lpar2* and *Lpar3*. At later ages (4 wk and 4 mo), *Lpar1* mRNA was detected in the inner tubules, tracking with waves of spermatogenesis, whereas *Lpar2* and *Lpar3* mRNA continued to be detected in early stage germ cells on the periphery of all seminiferous tubules (Fig. 1b). LPA receptor gene expression in male germ cells suggested that LPA signaling might affect spermatogenesis.

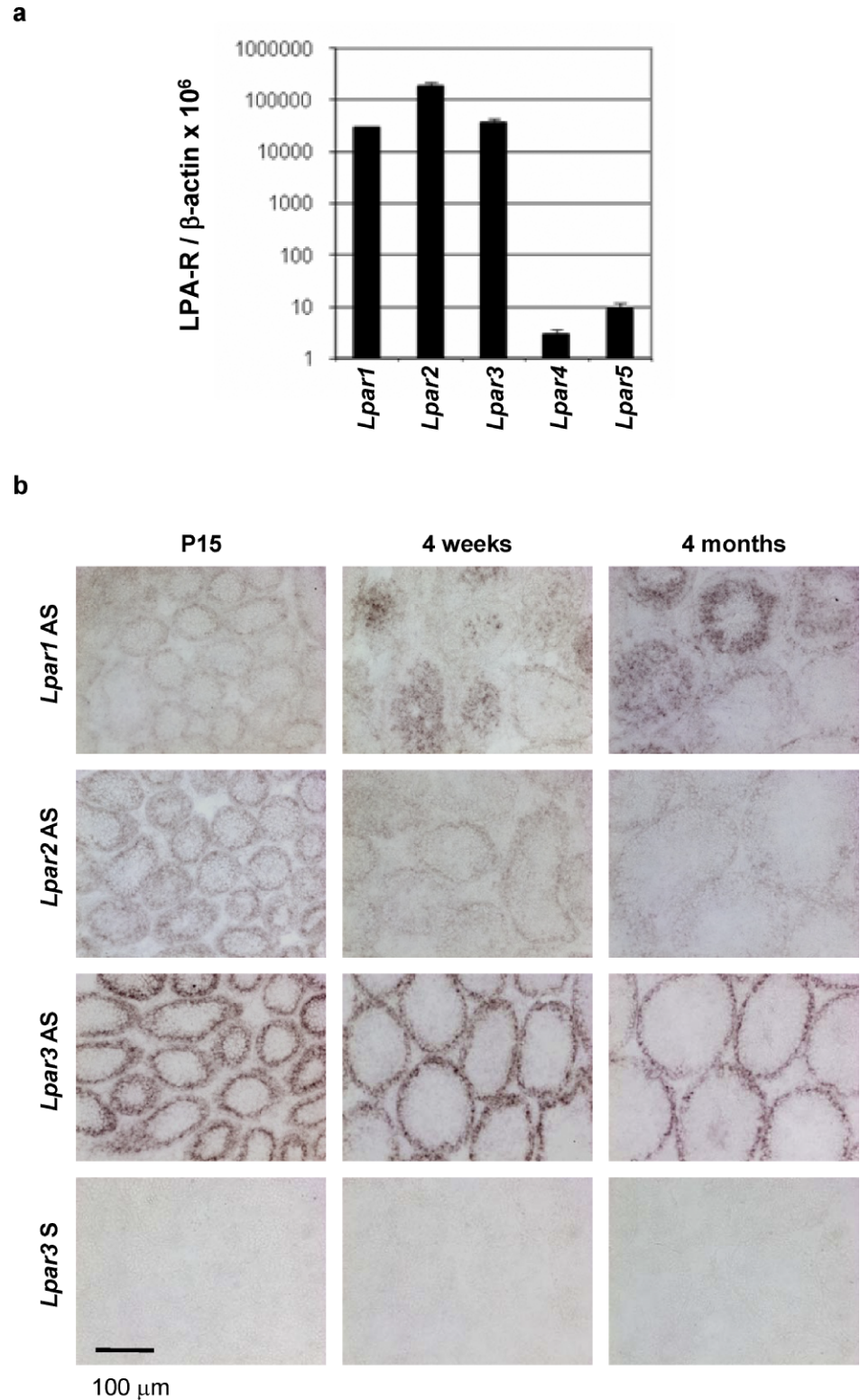
Testis Histology and Sperm Count in LPA Receptor Single- and Double-Null Mice

Although previous studies with *Lpar1*, *Lpar2*, or *Lpar3* single-knockout males did not reveal functional defects in male reproduction [17, 24, 25], we documented mild germ cell degeneration in the testes at 6 mo of age and a slight, but significant, reduction of sperm count from these single knockout males. *Lpar1/2*, *Lpar1/3*, and *Lpar2/3* double-knockout males had a further reduction of sperm count (Fig. 2a and data not shown). These results indicated that all three LPA receptors are involved in sperm production. Therefore, we focused on the *Lpar1/2/3* TKO testes.

General Characterization of Lpar1/2/3 TKO Mice

Lpar1/2/3 TKO mice have a number of phenotypes consistent with previously reported single-receptor deletants, such as reduced body weight, hematomas, and perinatal lethality, as seen in *Lpar1* mutants, as well as delayed implantation, prolonged pregnancy, and reduced litter size from *Lpar1/2/3* TKO females mated with WT males, as seen in *Lpar3* mutants (Fig. 2, b–d, and data not shown). Although *Lpar1/2/3* TKO females had phenotypes similar to those of *Lpar3* mutants in reproduction, more *Lpar1/2/3* TKO mice had hematomas compared with the LPA1 mutants: 41.2% (28 of 68) *Lpar1/2/3* TKO embryos (Embryonic Days 11.5–18.5) had

FIG. 1. Messenger RNA expression of LPA receptors in WT testis. **a)** Quantification by real-time RT-PCR of *Lpar1* through *Lpar5* in 4-wk-old testes ($n = 3$). Error bars represent the standard deviation. *Actb* was used as a loading control. **b)** In situ localization of *Lpar1*, *Lpar2*, and *Lpar3* in 15-day-, 4-wk-, and 4-mo-old testes. *Lpar3* sense probes were used as a negative control. AS, Antisense; S, sense. Bar = 100 μm .



hematomas, compared with 25.2% (31 of 123) in *Lpar1/2* double-mutant embryos (Embryonic Days 11.5–18.5), 26.5% (9 of 34) in *Lpar1/2* double-mutant neonatal pups, and 2.5% (4 of 160) in *Lpar1* mutant neonatal pups [25]. Interestingly, *Lpar2/3* double-mutant embryos (Embryonic Days 11.5–18.5) did not show hematomas (0 of 49). These results suggest that a receptor subtype compensation occurs via different LPA receptor combinations on hematomas, with a predominant predisposition produced by LPA1 loss. In addition, *Lpar1/2/3*

TKO mice showed more dramatic embryonic and postnatal lethality than did any of the single-null mice [17, 24, 25]. When *Lpar1/2/3* TKO males and females were crossed, they produced small litters (~2.8 pups/litter vs. 8 pups/litter in WT animals). Approximately 36% of the *Lpar1/2/3* TKO pups were born dead, compared with 2% in WT animals. In addition, 48% postnatal lethality in the *Lpar1/2/3* TKO pups, compared with 1% in WT animals, was observed. On average, only one *Lpar1/2/3* TKO pup per litter survived beyond 15 days of age

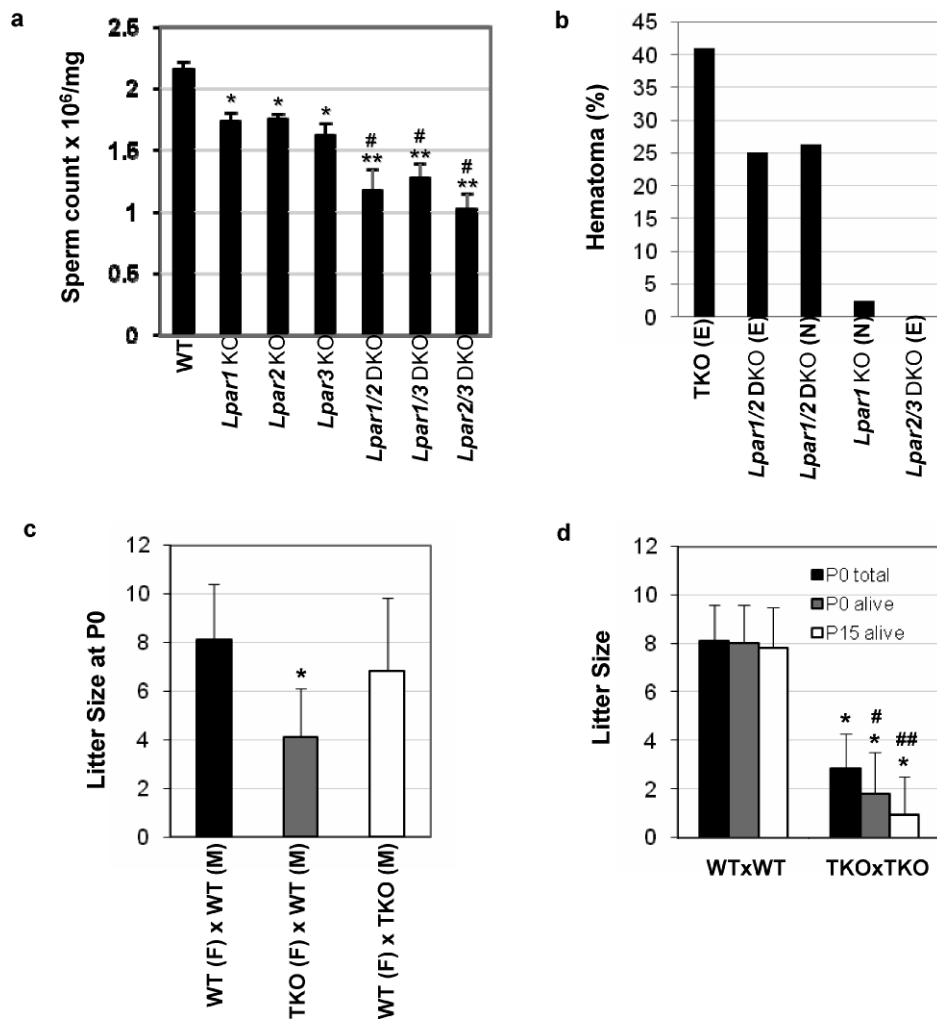


FIG. 2. Sperm count of *Lpar1*, *Lpar2*, and *Lpar3* single- and double-knockout (DKO) mice, occurrence of hematomas, and litter size of *Lpar1/2/3* TKO mice. **a**) Comparison of sperm count in the cauda epididymis of WT and *Lpar1*, *Lpar2*, and *Lpar3* single-null testes as well as *Lpar1/2*, *Lpar1/3*, and *Lpar2/3* double-null testes at 6-mo of age. Sperm count is expressed as sperm number per milligram of cauda epididymis. Error bars represent the SEM ($n = 5-10$). Two-tail unequal variance t -test: * $P < 0.005$, ** $P < 0.001$ vs. WT; # $P < 0.05$ vs. single nulls. **b**) Receptor-dependent occurrence of hematomas in embryos (E; Embryonic Days 11.5–18.5) and neonatal pups (N). **c**) Litter sizes from mating studies. The x-axis represents females (F) \times Males (M). Error bars represent the SD ($n = 12-26$). Two-tail unequal variance t -test: * $P = 1.00 \times 10^{-6}$. **d**) Litter size at Postnatal Day (P) 0 (total and alive) and P15 (alive) from WT \times WT ($n = 15$) and TKO \times TKO ($n = 114$) mating. Error bars represent the SD. Two-tail unequal variance t -test: * $P = 8.00 \times 10^{-12}$, 5.64×10^{-13} , and 5.03×10^{-13} , respectively, vs. WT; two-tail paired t -test: * $P = 2.61 \times 10^{-16}$ vs. *Lpar1/2/3* TKO P0 total; ** $P = 4.83 \times 10^{-11}$ vs. *Lpar1/2/3* TKO P0 alive.

(Fig. 2d). The TKO survivors gave us the opportunity to study the in vivo function of LPA signaling in male reproduction, with a focus on spermatogenesis.

Mating Activity

Lpar1/2/3 TKO young males (age 10–12 wk) were mated with 8-wk-old virgin WT females. These young TKO males only mated with two thirds of the females as indicated by plugs, whereas WT controls mated with 100% of females within the 1-mo mating period. These young TKO males also had a plugging latency nearly twice as long as that of WT controls. Plugging latency was the average time when the plug was found after cohabitation (Fig. 3a, b). As a result, these young TKO males had one third of the mating activity of WT controls. The females that developed plugs by mating with WT or TKO males, however, had similar pregnancy rates (Fig. 3c). In addition, no significant reduction of litter sizes was observed (Fig. 2c), indicating that the sperm from these young TKO males were functional and that the sperm numbers were not low enough to cause reduced litter size.

Testis Histology and Sperm Count

Lpar1/2/3 TKO testes showed age-related degenerative changes in the seminiferous tubules. At birth, the results of histological analyses of *Lpar1/2/3* TKO testes appeared to be grossly normal, although interstitial regions between tubules

were discernibly larger (Fig. 4a). At P15, abnormal tubular lumina and fewer spermatogonia and spermatocytes were observed in all *Lpar1/2/3* TKO testes examined (Fig. 4b). By 4 wk of age, all *Lpar1/2/3* TKO testes showed further reduction in cell numbers, along with increased vacuoles in seminiferous tubules (Fig. 4c). This phenotype became even more severe by 6 mo of age as the progressive accumulation of vacuoles destroyed the tubular architecture (Fig. 4d). Despite these changes, the *Lpar1/2/3* TKO adult testes did not show reduced weight. Instead, a slight but significantly higher weight increase compared with WT controls was found (Fig. 5a). Age-related degenerative changes in the testes of *Lpar1/2/3* TKO mice were paralleled by marked reductions in sperm count and increased rates of azoospermia. Sperm count from *Lpar1/2/3* TKO males was approximately 50% of controls at 2 mo and reduced to 18% of controls at 8 mo (Fig. 5b). This progressive reduction in sperm count occurred concomitantly with a progressive increase in azoospermic animals that reached 65% by 8 mo (Fig. 5c), the oldest age examined. LPA1/2/3-deficient sperm showed normal motility (data not shown), consistent with the results of mating studies.

Testosterone Levels

Spermatogenesis is controlled by both endocrine hormones and locally produced autocrine and paracrine factors [33, 34]. Testosterone is the major hormone regulating spermatogenesis;

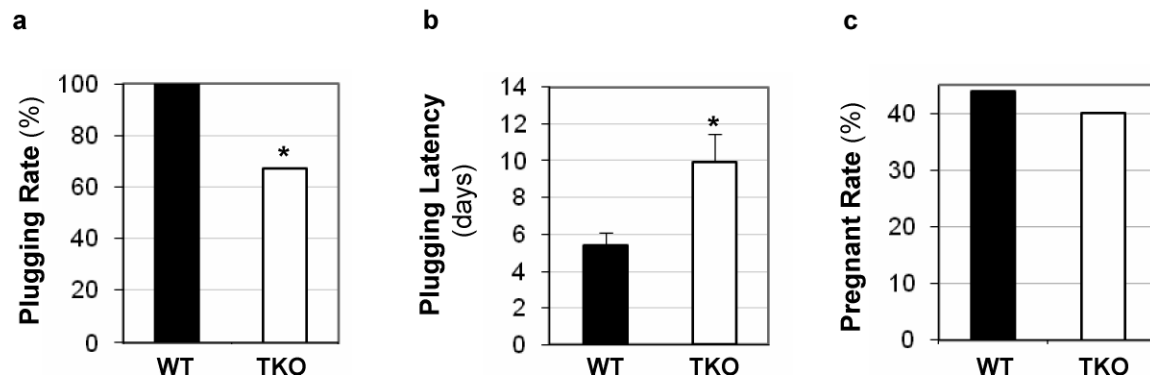


FIG. 3. Mating activity of *Lpar1/2/3* TKO mice. **a**) Plugging rate. WT: 57/57 = 100%; TKO: 30/45 = 66.7%. Chi-square test: * $P < 0.00005$. **b**) Plug latency. WT: $n = 30$; TKO, $n = 12$. Error bars represent the SEM. Two-tail unequal variance t -test: * $P \leq 0.05$. **c**) Pregnancy rate from plugged females. WT: 25/57 = 43.3%, TKO: 12/30 = 40%.

therefore, we assessed serum testosterone levels in *Lpar1/2/3* TKO males. No significant differences were observed between 3 and 6 mo (median, 0.43 ng/ml; range, 0.15–13.69 ng/ml; $n = 19$) compared with age-matched WT controls (median, 0.39 ng/ml; range, 0.22–11.76 ng/ml; $n = 24$). These data indicate that spermatogenic defects in *Lpar1/2/3* TKO males likely are the result of local LPA receptor-mediated signaling influences in the seminiferous tubules rather than systemic changes in endocrine function.

MAPK3/1 Phosphorylation

It has been shown previously that LPA can promote cell survival and proliferation through receptor activation of the heterotrimeric G protein, $G_{i/o}$ [1, 35–37]. Figure 6a showed the time course and dose–response of LPA-induced MAPK3/1 phosphorylation in the control testicular primary cells. The LPA-induced, $G_{i/o}$ -mediated phosphorylation of MAPK3/1 was completely abolished in testicular primary cells from *Lpar1/2/3* TKO mice, whereas MAPK3/1 phosphorylation induced by another lysophospholipid, sphingosine 1-phosphate, was not affected (Fig. 6b).

Germ Cell Apoptosis

Loss of $G_{i/o}$ -mediated LPA signaling was accompanied by increased germ cell apoptosis in the *Lpar1/2/3* TKO testes. Apoptotic germ cells detected by ISEL⁺ were present throughout the seminiferous tubules of both WT and *Lpar1/2/3* TKO testes (Fig. 7a) [29]. The percentages of ISEL⁺-labeled germ cells, however, were significantly increased in *Lpar1/2/3* TKO testes at all ages examined (15 days, 3 mo, and 8 mo) (Fig. 7b), indicating increased germ cell apoptosis in the *Lpar1/2/3* TKO testes.

Germ Cell Proliferation

The same testes also were examined for germ cell proliferation as assessed by BrdU incorporation and immunolabeling. The BrdU-labeled germ cells were detected throughout the seminiferous tubules at 15 days of age and were restricted to the proliferating spermatogonia (in the periphery of the seminiferous tubules) in adult testes (Fig. 8a). Semiquantitative analyses demonstrated a reduced percentage of tubules with BrdU labeling in the 3- and 8-mo *Lpar1/2/3* TKO testes, indicating that germ cell proliferation was significantly reduced in adult *Lpar1/2/3* TKO testes. No reduction of germ cell proliferation, however, was observed in 15-day-old *Lpar1/2/3* TKO testes (Fig. 8b). These data suggest that the reduction of germ cell proliferation in *Lpar1/2/3* TKO seminiferous tubules is a secondary effect of increased germ cell apoptosis.

DISCUSSION

The three closely related LPA receptors, *Lpar1*, *Lpar2*, and *Lpar3*, have similar expression patterns in the testes before puberty. The expression of *Lpar1*, however, changes between

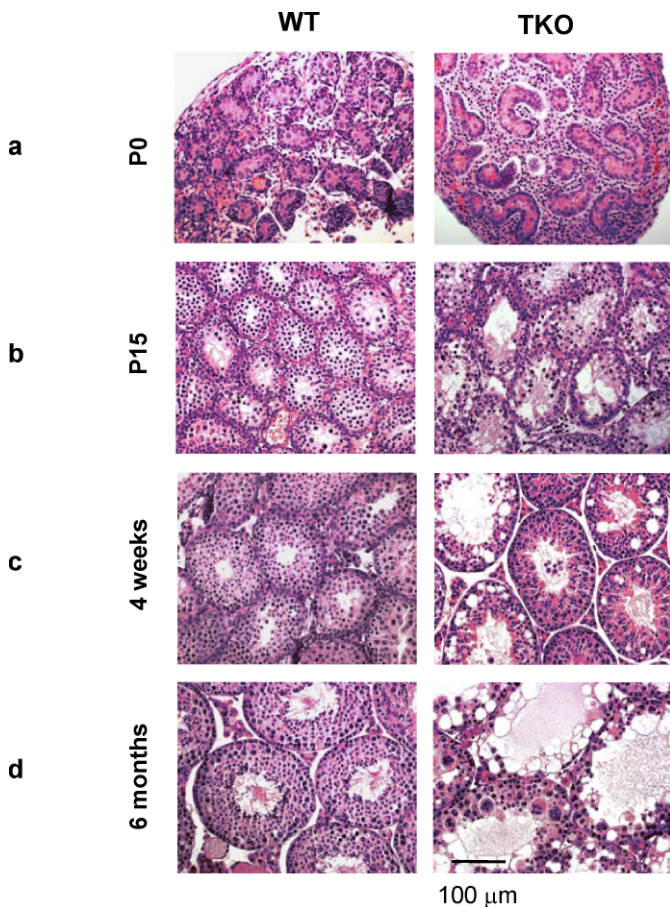


FIG. 4. Histology of *Lpar1/2/3* TKO testes during development: (a) Postnatal Day (P) 0, (b) P15, (c) 4 wk; (d) 6 mo. Paraffin sections (thickness, 5 μ m) were cut and stained with hematoxylin and eosin. Bar = 100 μ m.

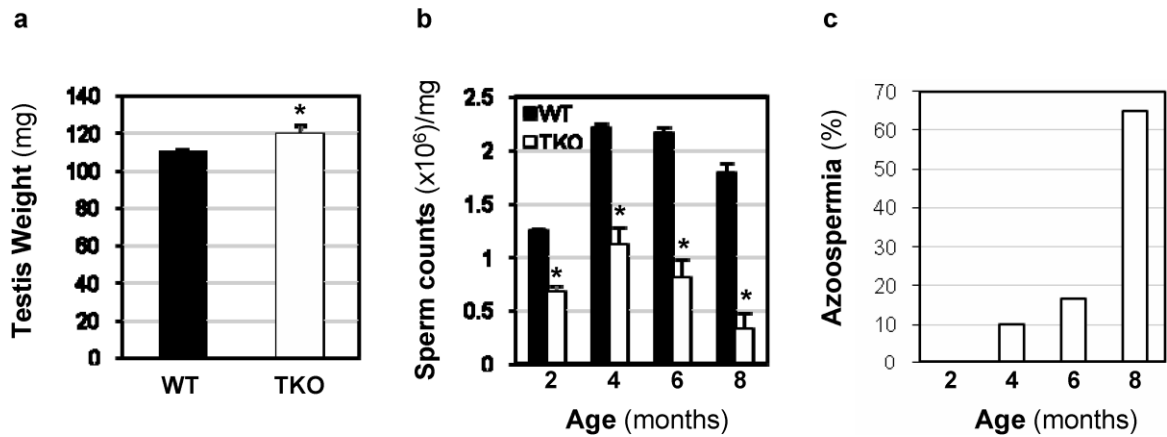


FIG. 5. Testis weight and sperm count of *Lpar1/2/3* TKO males. **a**) Testis weight. Two-tail unequal variance *t*-test: * $P < 0.05$. **b**) Comparison of sperm counts in the cauda epididymis of WT and *Lpar1/2/3* TKO mice at 2, 4, 6, and 8 mo of age. Sperm count is expressed as sperm number $\times 10^6$ per milligram of cauda epididymis. Error bars represent the SEM ($n = 5-16$). Two-tail unequal variance *t*-test: * $P < 0.0005$. **c**) The percentage of *Lpar1/2/3* TKO testes with azoospermia ($n = 10-20$).

puberty and adulthood, resembling the expression pattern of the growth factor bone morphogenetic proteins (BMPs) *Bmp7* and *Bmp8*, the expression patterns of which are stage specific [38]. *Lpar2* and *Lpar3* are constitutively expressed in the basal regions of seminiferous tubules, primarily in immature germ cells, such as spermatogonia and spermatocytes, and are undetectable in elongating spermatids or mature spermatozoa (Fig. 1b). This expression pattern is similar to that of *Bcl2l2* (*Bcl-w*) [39]. Interestingly, disruption of BMP7 and BMP8 or BCL2L2 also results in impaired spermatogenesis [38, 39]. The stage-specific expression of *Lpar1* in germ cells and the apparent constitutive expression of the *Lpar2* and *Lpar3* in spermatogonial and early spermatocytes suggest that LPA may play multiple and convergent roles through different receptors in promoting germ cell development.

The potential roles of LPA in spermatogenesis are manifested by the histological changes in the testes of LPA

receptor(s) KO mice (Fig. 4 and data not shown). The tubules are not affected at the same time and rate; however, this heterogeneity in spermatogenic disruption also is apparent in other knockout models [39–41]. Despite this heterogeneity, vacuolar degeneration was seen in all the TKO testes. This degeneration is progressive, and by 8 mo of age, the degeneration results in azoospermia in most males. Defects in spermatogenesis appear to be the result of a direct effect on germ cell development and are distinct from indirect effects, as seen in *Esr1* (*ER α*) knockout mice, in which male infertility was caused by the interruption of luminal fluid in the head of epididymis [42]. Loss of germ cells usually leads to testicular atrophy [43, 44], yet interestingly, the TKO testes had an average mass comparable to that of age-matched WT testes. This may reflect a defect in luminal fluid absorption in the TKO mice, resulting in retained fluid and maintained testicular mass.

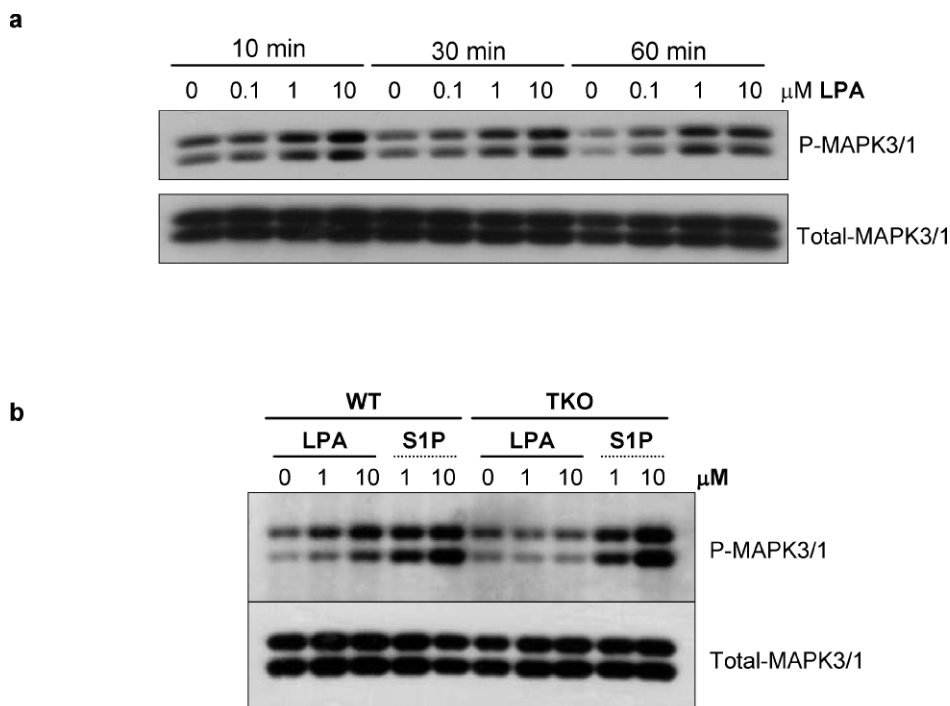


FIG. 6. MAPK3/1 phosphorylation in *Lpar1/2/3* TKO testicular primary cells. **a**) Dose response and time course of LPA-induced MAPK3/1 phosphorylation in control testis primary cells. **b**) Loss of LPA-induced MAPK3/1 phosphorylation in *Lpar1/2/3* TKO testicular primary cells measured after LPA and sphingosine 1-phosphate (S1P) treatment for 10 min.

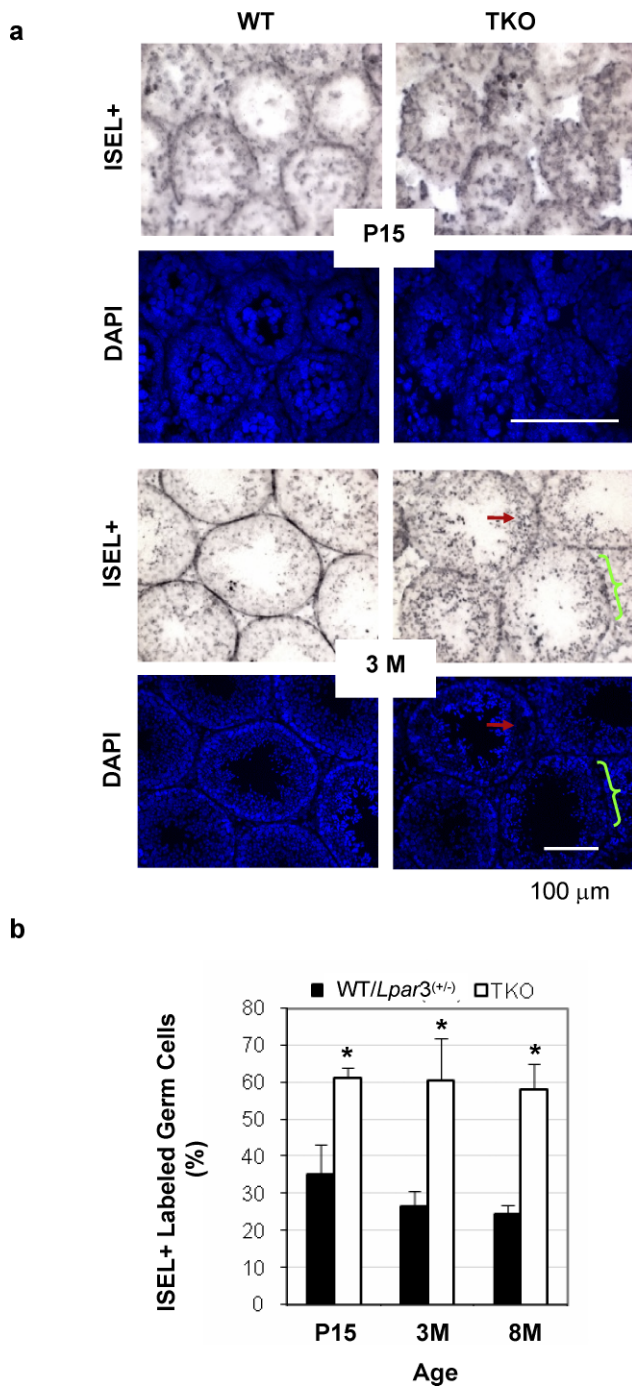


FIG. 7. Germ cell apoptosis in *Lpar1/2/3* TKO testes. **a**) ISEL⁺ detection of apoptotic cells in WT and *Lpar1/2/3* TKO testes at Postnatal Day (P) 15 and 3 mo (3M). Red arrows indicate apoptotic germ cells. Green brackets indicate apoptotic spermatogonia. **b**) Percentages of apoptotic germ cells in control and *Lpar1/2/3* TKO testes at P15, 3M, and 8 mo (8M). Error bars represent the SD (n = 4–8). Two-tail unequal variance *t*-test: **P* < 0.05. Bar = 100 μ m.

The deletion of *Lpar1*, *Lpar2*, and *Lpar3* affects male reproductive function in at least two ways: reduced mating activity, and an age-related increase of sterile males. Even at the peak of fertility (age, ~3 mo), the copulation frequency of TKO mice as a population was approximately one third that of age- and background-matched WT controls (Fig. 3a, b). Reduced mating activity also has been reported in *ER* and *Bcl6* knockout mice [41, 45]. The *Lpar1/2/3* TKO males,

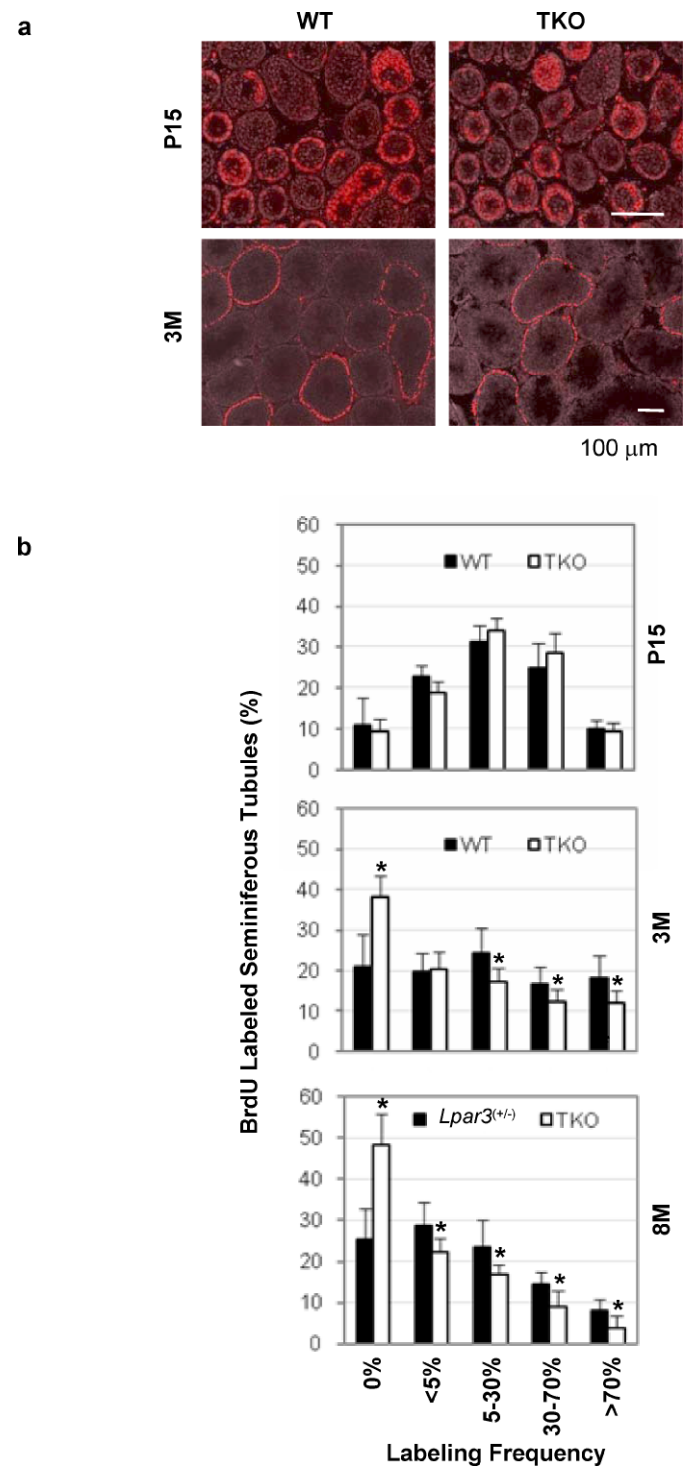


FIG. 8. Germ cell proliferation in *Lpar1/2/3* TKO testes. **a**) BrdU detection of proliferating germ cells in WT and *Lpar1/2/3* TKO testes at Postnatal Day (P) 15 and 3 mo (3M). **b**) Semiquantification of germ cell proliferation at P15, 3M, and 8 mo (8M). Error bars represent the SD (n = 4–8). At P15, no significant differences were found. Two-tail unequal variance *t*-test: **P* < 0.05. Bar = 100 μ m.

however, do not initially produce significantly smaller litters, suggesting that early sperm reduction (~50% at ~3 mo of age) is not sufficient to affect the litter size, similar to what has been reported in *Arl4a*, centromere protein B, or testis-specific cytochrome *c* knockout mice [43, 46, 47]. A study with *Fshb* and activin receptor IIA knockout mice indicated that a sperm

reduction to 8% of that in WT animals was needed to reduce litter sizes to 50% of those for WT animals. The litter size was not affected even when the sperm count was 27% of that in WT animals [48].

Spermatogenesis is controlled by endocrine and local (paracrine/autocrine) signals [49]. With no change in testosterone level in the TKO mice, the documented role of LPA itself as a paracrine/autocrine mediator in other systems [37] suggests that impaired spermatogenesis in the LPA receptor(s) KO males is caused by local LPA signaling defects that affect cell proliferation and/or apoptosis. A similar effect also was seen in Schwann cells of the peripheral nervous system [50]. It has been established that germ cell degeneration limits spermatogenesis and that survival factor deprivation leads to apoptosis [51]. Furthermore, the phenotype is consistent with the antiapoptotic effects of LPA that involve $G_{i/o}$ signaling [35, 36] and includes activation of AKT1 [50]. Because LPA-induced $G_{i/o}$ signaling was impaired in *Lpar1/2/3* TKO testis primary cells (Fig. 6b), LPA1, LPA2, and/or LPA3, coupled at least to $G_{i/o}$ signaling, can account for the germ cell survival effects of LPA. The potential roles of other G proteins and their downstream signaling pathways that mediate the survival effect of LPA on male germ cells require further study. The results presented here thus implicate LPA as a novel lipid factor influencing spermatogenesis through its signaling effects on germ cell survival.

The endogenous source of LPA is likely to be local rather than through the bloodstream. This interpretation is supported by studies with transgenic mice that ubiquitously overexpressed phosphatidic acid phosphatase 2a (PPAP2A; or lipid phosphate phosphatase-1 [LPP-1]), an enzyme that degrades LPA, and that showed disrupted spermatogenesis without affecting bloodborne LPA levels [52]. The presence of LPA and LPA metabolic enzymes in human seminal fluid [21] suggests that LPA signaling may have similar roles in human spermatogenesis.

To our knowledge, the present study is the first to identify receptor-mediated lysophospholipid signaling as an important factor in maintaining mating activity and normal sperm production via three identified receptors, LPA1, LPA2, and LPA3. Many issues remain to be explored. These include the source(s) of signaling LPA and LPA metabolism, involvement of other LPA receptors (both known and unknown), actual downstream signaling pathways, intersections with other signaling pathways, and neural mechanisms associated with behavioral deficits. Additionally, the age-related progression of germ cell degeneration associated with loss of LPA signaling suggests a temporal window during which sperm production could be pharmaceutically altered. Thus, LPA drug-based therapies could potentially result in new treatment options for male infertility or a new contraceptive strategy. Combined with previous data regarding female reproductive functions [17], these results underscore pivotal roles for LPA signaling in mammalian reproduction through defined receptor subtypes.

ACKNOWLEDGMENTS

We thank J.J.A. Contos, C. McGiffert, S. Kawamura, S. Miyamoto, J.H. Brown, I. Sadler-Riggelman, M.A. Kingsbury, C. Akita, Y. Yung, J.W. Westra, C. Paczkowski, D.R. Herr, and D. Letourneau for technical assistance and critical reading of the manuscript.

REFERENCES

- Ishii I, Fukushima N, Ye X, Chun J. Lysophospholipid receptors: signaling and biology. *Annu Rev Biochem* 2004; 73:321–354.
- Budnik LT, Mukhopadhyay AK. Lysophosphatidic acid and its role in reproduction. *Biol Reprod* 2002; 66:859–865.
- Fukushima N, Ishii I, Contos JJ, Weiner JA, Chun J. Lysophospholipid receptors. *Annu Rev Pharmacol Toxicol* 2001; 41:507–534.
- Gaits F, Fourcade O, Le Balle F, Gueguen G, Gaige B, Gassama-Diagne A, Fauvel J, Salles JP, Mauco G, Simon MF, Chap H. Lysophosphatidic acid as a phospholipid mediator: pathways of synthesis. *FEBS Lett* 1997; 410:54–58.
- Xu Y, Xiao YJ, Zhu K, Baudhuin LM, Lu J, Hong G, Kim KS, Cristina KL, Song L, Williams FS, Elson P, Markman M, Belinson J. Unfolding the pathophysiological role of bioactive lysophospholipids. *Curr Drug Targets Immune Endocr Metab Disord* 2003; 3:23–32.
- Aoki J. Mechanisms of lysophosphatidic acid production. *Semin Cell Dev Biol* 2004; 15:477–489.
- Gesta S, Simon MF, Rey A, Sibrac D, Girard A, Lafontan M, Valet P, Saulnier-Blache JS. Secretion of a lysophospholipase D activity by adipocytes: involvement in lysophosphatidic acid synthesis. *J Lipid Res* 2002; 43:904–910.
- Pebay A, Bonder CS, Pitson SM. Stem cell regulation by lysophospholipids. *Prostaglandins Other Lipid Mediat* 2007; 84:83–97.
- Lee CW, Rivera R, Gardell S, Dubin AE, Chun J. GPR92 as a new G12/13- and Gq-coupled lysophosphatidic acid receptor that increases cAMP, LPA5. *J Biol Chem* 2006; 281:23589–23597.
- Kotarsky K, Boketoft A, Bristulf J, Nilsson NE, Norberg A, Hansson S, Owman C, Sillard R, Leeb-Lundberg LM, Olde B. Lysophosphatidic acid binds to and activates GPR92, a G protein-coupled receptor highly expressed in gastrointestinal lymphocytes. *J Pharmacol Exp Ther* 2006; 318:619–628.
- Ye X, Fukushima N, Kingsbury MA, Chun J. Lysophosphatidic acid in neural signaling. *Neuroreport* 2002; 13:2169–2175.
- Siess W, Tigyi G. Thrombogenic and atherogenic activities of lysophosphatidic acid. *J Cell Biochem* 2004; 92:1086–1094.
- Chun J. Lysophospholipids in the nervous system. *Prostaglandins Other Lipid Mediat* 2005; 77:46–51.
- Gardell SE, Dubin AE, Chun J. Emerging medicinal roles for lysophospholipid signaling. *Trends Mol Med* 2006; 12:65–75.
- Lin DA, Boyce JA. Lysophospholipids as mediators of immunity. *Adv Immunol* 2006; 89:141–167.
- Watterson KR, Lanning DA, Diegelmann RF, Spiegel S. Regulation of fibroblast functions by lysophospholipid mediators: potential roles in wound healing. *Wound Repair Regen* 2007; 15:607–616.
- Ye X, Hama K, Contos JJ, Anliker B, Inoue A, Skinner MK, Suzuki H, Amano T, Kennedy G, Arai H, Aoki J, Chun J. LPA3-mediated lysophosphatidic acid signaling in embryo implantation and spacing. *Nature* 2005; 435:104–108.
- Higgs HN, Glomset JA. Purification and properties of a phosphatidic acid-preferring phospholipase A_1 from bovine testis: examination of the molecular basis of its activation. *J Biol Chem* 1996; 271:10874–10883.
- Ito M, Tchoua U, Okamoto M, Tojo H. Purification and properties of a phospholipase A_2 /lipase preferring phosphatidic acid, bis(monoacylglycerol) phosphate, and monoacylglycerol from rat testis. *J Biol Chem* 2002; 277:43674–43681.
- Lee HY, Murata J, Clair T, Polymeropoulos MH, Torres R, Manrow RE, Liotta LA, Stracke ML. Cloning, chromosomal localization, and tissue expression of autotaxin from human teratocarcinoma cells. *Biochem Biophys Res Commun* 1996; 218:714–719.
- Sonoda H, Aoki J, Hiramatsu T, Ishida M, Bandoh K, Nagai Y, Taguchi R, Inoue K, Arai H. A novel phosphatidic acid-selective phospholipase A_1 that produces lysophosphatidic acid. *J Biol Chem* 2002; 277:34254–34263.
- Xie Y, Meier KE. Lysophospholipase D and its role in LPA production. *Cell Signal* 2004; 16:975–981.
- Contos JJ, Ishii I, Chun J. Lysophosphatidic acid receptors. *Mol Pharmacol* 2000; 58:1188–1196.
- Contos JJ, Fukushima N, Weiner JA, Kaushal D, Chun J. Requirement for the lpA1 lysophosphatidic acid receptor gene in normal suckling behavior. *Proc Natl Acad Sci U S A* 2000; 97:13384–13389.
- Contos JJ, Ishii I, Fukushima N, Kingsbury MA, Ye X, Kawamura S, Brown JH, Chun J. Characterization of lpa(2) (Edg4) and lpa(1)/lpa(2) (Edg2/Edg4) lysophosphatidic acid receptor knockout mice: signaling deficits without obvious phenotypic abnormality attributable to lpa(2). *Mol Cell Biol* 2002; 22:6921–6929.
- McGiffert C, Contos JJ, Friedman B, Chun J. Embryonic brain expression analysis of lysophospholipid receptor genes suggests roles for s1p(1) in neurogenesis and s1p(1–3) in angiogenesis. *FEBS Lett* 2002; 531:103–108.
- Weiner JA, Hecht JH, Chun J. Lysophosphatidic acid receptor gene *vzg-1/lpA1/edg-2* is expressed by mature oligodendrocytes during myelination in the postnatal murine brain. *J Comp Neurol* 1998; 398:587–598.

28. Kawamura S, Miyamoto S, Brown JH. Initiation and transduction of stretch-induced RhoA and Rac1 activation through caveolae: cytoskeletal regulation of ERK translocation. *J Biol Chem* 2003; 278:31111–31117.
29. Blaschke AJ, Staley K, Chun J. Widespread programmed cell death in proliferative and postmitotic regions of the fetal cerebral cortex. *Development* 1996; 122:1165–1174.
30. Hecht JH, Weiner JA, Post SR, Chun J. Ventricular zone gene-1 (vzg-1) encodes a lysophosphatidic acid receptor expressed in neurogenic regions of the developing cerebral cortex. *J Cell Biol* 1996; 135:1071–1083.
31. Kingsbury MA, Rehen SK, Contos JJ, Higgins CM, Chun J. Non-proliferative effects of lysophosphatidic acid enhance cortical growth and folding. *Nat Neurosci* 2003; 6:1292–1299.
32. Lee CW, Rivera R, Dubin AE, Chun J. LPA(4)/GPR23 is a lysophosphatidic acid (LPA) receptor utilizing G(s)-, G(q)/G(i)-mediated calcium signaling and G(12/13)-mediated Rho activation. *J Biol Chem* 2007; 282:4310–4317.
33. Cooke HJ, Saunders PT. Mouse models of male infertility. *Nat Rev Genet* 2002; 3:790–801.
34. O'Bryan MK, de Kretser D. Mouse models for genes involved in impaired spermatogenesis. *Int J Androl* 2006; 29:76–89 [discussion 105–108].
35. Moolenaar WH. Development of our current understanding of bioactive lysophospholipids. *Ann N Y Acad Sci* 2000; 905:1–10.
36. Ye X, Ishii I, Kingsbury MA, Chun J. Lysophosphatidic acid as a novel cell survival/apoptotic factor. *Biochim Biophys Acta* 2002; 1585:108–113.
37. Xie Y, Gibbs TC, Meier KE. Lysophosphatidic acid as an autocrine and paracrine mediator. *Biochim Biophys Acta* 2002; 1582:270–281.
38. Zhao GQ, Chen YX, Liu XM, Xu Z, Qi X. Mutation in *Bmp7* exacerbates the phenotype of *Bmp8a* mutants in spermatogenesis and epididymis. *Dev Biol* 2001; 240:212–222.
39. Print CG, Loveland KL, Gibson L, Meehan T, Stylianou A, Wreford N, de Kretser D, Metcalf D, Kontgen F, Adams JM, Cory S. Apoptosis regulator *bcl-w* is essential for spermatogenesis but appears otherwise redundant. *Proc Natl Acad Sci U S A* 1998; 95:12424–12431.
40. Robertson KM, O'Donnell L, Jones ME, Meachem SJ, Boon WC, Fisher CR, Graves KH, McLachlan RI, Simpson ER. Impairment of spermatogenesis in mice lacking a functional aromatase (*cyp19*) gene. *Proc Natl Acad Sci U S A* 1999; 96:7986–7991.
41. Eddy EM, Washburn TF, Bunch DO, Goulding EH, Gladen BC, Lubahn DB, Korach KS. Targeted disruption of the estrogen receptor gene in male mice causes alteration of spermatogenesis and infertility. *Endocrinology* 1996; 137:4796–4805.
42. Hess RA, Bunick D, Lee KH, Bahr J, Taylor JA, Korach KS, Lubahn DB. A role for estrogens in the male reproductive system. *Nature* 1997; 390:509–512.
43. Narisawa S, Hecht NB, Goldberg E, Boatright KM, Reed JC, Millan JL. Testis-specific cytochrome *c*-null mice produce functional sperm but undergo early testicular atrophy. *Mol Cell Biol* 2002; 22:5554–5562.
44. Zindy F, van Deursen J, Grosveld G, Sherr CJ, Roussel MF. *INK4d*-deficient mice are fertile despite testicular atrophy. *Mol Cell Biol* 2000; 20:372–378.
45. Kojima S, Hatano M, Okada S, Fukuda T, Toyama Y, Yuasa S, Ito H, Tokuhisa T. Testicular germ cell apoptosis in *Bcl6*-deficient mice. *Development* 2001; 128:57–65.
46. Schurmann A, Koling S, Jacobs S, Saftig P, Krauss S, Wennemuth G, Kluge R, Joost HG. Reduced sperm count and normal fertility in male mice with targeted disruption of the ADP-ribosylation factor-like 4 (*Arl4*) gene. *Mol Cell Biol* 2002; 22:2761–2768.
47. Hudson DF, Fowler KJ, Earle E, Saffery R, Kalitsis P, Trowell H, Hill J, Wreford NG, de Kretser DM, Cancilla MR, Howman E, Hii L, et al. Centromere protein B null mice are mitotically and meiotically normal but have lower body and testis weights. *J Cell Biol* 1998; 141:309–319.
48. Kumar TR, Varani S, Wreford NG, Telfer NM, de Kretser DM, Matzuk MM. Male reproductive phenotypes in double mutant mice lacking both *FSHbeta* and activin receptor IIA. *Endocrinology* 2001; 142:3512–3518.
49. Print CG, Loveland KL. Germ cell suicide: new insights into apoptosis during spermatogenesis. *Bioessays* 2000; 22:423–430.
50. Weiner JA, Chun J. Schwann cell survival mediated by the signaling phospholipid lysophosphatidic acid. *Proc Natl Acad Sci U S A* 1999; 96:5233–5238.
51. Sinha Hikim AP, Swerdloff RS. Hormonal and genetic control of germ cell apoptosis in the testis. *Rev Reprod* 1999; 4:38–47.
52. Yue J, Yokoyama K, Balazs L, Baker DL, Smalley D, Pilquill C, Brindley DN, Tigyi G. Mice with transgenic overexpression of lipid phosphate phosphatase-1 display multiple organotypic deficits without alteration in circulating lysophosphatidate level. *Cell Signal* 2004; 16:385–399.